Journal of Applied Mathematics and Physics (ZAMP)
Vol. 27, 1976 Birkhäuser Verlag Basel

Magnetohydrodynamic Free Convection About a Semi-infinite Vertical Plate in a Strong Cross Field

By Graham Wilks, Dept. of Mathematics, University of Strathclyde, Glasgow, Great Britain

1. Introduction

In this paper we examine the simultaneous occurrence of buoyancy and magnetic forces in the flow of an electrically conducting fluid up a hot vertical plate in a strong cross-magnetic field. Singh and Cowling [1] have shown that regardless of the strength of the applied magnetic field there will always be a region in the neighbourhood of the leading edge of the plate where electromagnetic forces are unimportant, whilst at large distances from the leading edge these magnetic forces dominate. The flow near the leading edge has been examined by Sparrow and Cess [2] whilst Singh and Cowling focussed their attention on conditions downstream. In particular they concentrated on examining that outer region of the boundary layer, which must always ultimately appertain, in which an inviscid balance between buoyancy and magnetic forces is achieved. Subsequent authors, Riley [3] and Kuiken [4] have re-examined the problem with a view to incorporating in the solution the inner viscous layer within the downstream boundary layer which is appropriate if the boundary condition of 'no slip' at the plate is to be satisfied. Their attempts to use the method of matched asymptotic expansions in terms of a non-dimensional parameter in this region encountered difficulties associated with the asymptotic nature of the solution in respect of an unknown location of the leading edge.

The work that follows reformulates the problem in terms of coordinate expansions with respect to a non-dimensional characteristic length which is fundamental to the problem in its reflection of the relative magnitudes of the buoyancy and magnetic forces at varying locations along the plate. This formulation provides the basis for a complete numerical integration from the leading edge which for the first time provides details of skin friction and heat transfer coefficients at all stations along the plate. Moreover an estimate may be made of an indeterminacy in asymptotic solutions which allows favourable comparison to be made between series solution estimates of skin friction and heat transfer and their exact numerical values.

2. The Problem

Consider the free convection flow of an electrically conducting, non-magnetic fluid up a heated semi-infinite plate extending vertically upwards with its leading edge

horizontal. The plate is maintained at a constant temperature T_0, greater than the constant temperature T_∞ of the surrounding fluid, in the presence of a strong magnetic field H_0 normal to the plate. The magnetic Reynolds number $R_m = 4\pi\kappa\sigma$ where κ is the thermal diffusivity and σ the electrical conductivity of the fluid is taken to be small compared to unity allowing neglect of perturbations to the basic normal field. Fluid property variations are limited to a density variation which is taken into account only insofar as it affects the buoyancy terms, i.e. the Boussinesq approximation is applicable throughout. The reference density ρ_∞ is taken as that of the surrounding ambient fluid. Neglect of viscous and electrical dissipation together with the short circuit assumption has been shown by previous authors to give rise to the governing dimensional equations expressing conservation of momentum, energy and mass as

$$u\frac{\partial u}{\partial x} + v\frac{\partial u}{\partial y} = g\beta(T - T_\infty) - \sigma\frac{H_0^2}{\rho_\infty}u + \nu\frac{\partial^2 u}{\partial y^2} \tag{1}$$

$$u\frac{\partial T}{\partial x} + v\frac{\partial T}{\partial y} = \frac{\partial^2 T}{\partial y^2} \tag{2}$$

$$\frac{\partial u}{\partial x} + \frac{\partial v}{\partial y} = 0 \tag{3}$$

to be solved subject to the boundary conditions

$$\begin{aligned} &u = v = 0, \quad T = T_0 \quad \text{at } y = 0 \\ &u \to 0, \quad T \to T_\infty \quad \text{as } y \to \infty \\ &\left.\begin{aligned} u &= 0 \\ T &= T_\infty \end{aligned}\right\} \quad \text{at } x = 0,\ y > 0. \end{aligned} \tag{4}$$

Here (u, v) are velocity components associated with the directions of increasing coordinates (x, y) measured along and normal to the plate respectively. T is the temperature, g the acceleration due to gravity, β the coefficient of thermal expansion and ν the kinematic viscosity of the fluid.

With respect to a characteristic length L the following non-dimensional quantities are in evidence

$$\mathrm{Gr}_\nu = \frac{g\beta(T_0 - T_\infty)L^3}{\nu^2}, \quad \text{Grashof number}$$

$$\mathrm{Gr}_\kappa = \frac{g\beta(T_0 - T_\infty)L^3}{\kappa^2}, \quad \text{Modified Grashof number}$$

$$H_\nu = \left(\frac{\sigma H_0^2}{\rho_\infty \nu}\right)^{1/2} L, \quad \text{Hartmann number}$$

$$H_\kappa = \left(\frac{\sigma H_0^2}{\rho_\infty \kappa}\right) L, \quad \text{Modified Hartmann number}$$

$$\mathrm{Pr} = \frac{\nu}{\kappa}, \quad \text{Prandtl number}$$

Since the geometry under consideration lacks an obvious length scale non-dimensional

parameters are best considered as local parameters with respect to the distance from the leading edge x. This local variation of parameters reflecting the relative magnitudes of the forces involved at a given station is instrumental in formulating the problem in a form suitable for numerical integration. In particular the non-dimensional quantity

$$\xi = \frac{(\sigma H_0^2/\rho_\infty)^2}{g\beta(T_0 - T_\infty)}\, x = \frac{H_{v,\,x}^4}{\mathrm{Gr}_{v,\,x}} = \frac{H_{\kappa,\,x}^4}{\mathrm{Gr}_{\kappa,\,x}} \tag{5}$$

represents a local measure of the relative magnitude of magnetic and buoyancy forces independent of viscous or thermal diffusion elements. Consequently we seek to formulate the problem in terms of this fundamental dimensionless characteristic coordinate.

The semi-infinite problem may now be examined as a combination of a direct coordinate expansion for small ξ (near the leading edge) and an inverse coordinate expansion for large ξ (downstream) whose regions of validity may be gauged via comparison with a full numerical solution.

3. I. Series solution near the leading edge—small ξ

Transformations appropriate in this vicinity are

$$\begin{aligned} \psi &= 4c\kappa x^{3/4}\phi(\xi, \eta) \\ T - T_\infty &= (T_0 - T_\infty)\theta(\xi, \eta) \\ \eta &= \frac{cy}{x^{1/4}}, \qquad c = \left[\frac{g\beta(T_0 - T_\infty)}{4\kappa^2}\right]^{1/4}. \end{aligned} \tag{6}$$

On substitution in the governing equations (1)–(3) these yield

$$\mathrm{Pr}\,\phi_{\eta\eta\eta} + 3\phi\phi_{\eta\eta} - 2\phi_\eta^2 + \theta - 2\xi^{1/2}\phi_\eta = 4\xi\{\phi_\eta\phi_{\eta\xi} - \phi_\xi\phi_{\eta\eta}\} \tag{7}$$

$$\theta_{\eta\eta} + 3\phi\theta_\eta = 4\xi\{\theta_\eta\theta_\xi - \phi_\xi\theta_\eta\} \tag{8}$$

to be solved subject to the boundary conditions

$$\begin{aligned} \phi = 0, \quad \frac{\partial\phi}{\partial\eta} = 0; \qquad & \theta = 1 \quad \text{on } \eta = 0 \\ \frac{\partial\phi}{\partial\eta} \to 0; \qquad & \theta \to 0 \quad \text{as } \eta \to \infty \\ \theta = \frac{\partial\phi}{\partial\eta} = 0 \quad & \text{at } \xi = 0,\ \eta > 0. \end{aligned} \tag{9}$$

The direct coordinate expansion solutions in powers of $\xi^{1/2}$ are

$$\begin{aligned} \phi(\xi, \eta) &= \phi_0(\eta) + \xi^{1/2}\phi_1(\eta) + \xi\phi_2(\eta) + \cdots \\ \theta(\xi, \eta) &= \theta_0(\eta) + \xi^{1/2}\theta_1(\eta) + \xi\theta_2(\eta) + \cdots \end{aligned} \tag{10}$$

where ϕ_0, θ_0 are the well-known free convection similarity solutions for flow around a constant temperature semi-infinite vertical plate, extensively studied by Ostrach [5], and where ϕ_1, θ_1 are effectively the first-order corrections to the flow due to the

presence of the magnetic field. ϕ_1, θ_1 may be directly inferred from the numerical solutions of Sparrow and Cess.

4. II. Series solution downstream—large ξ

4.1. Outer Layer

Transformations reflecting the effective balance between buoyancy and magnetic forces in this region are

$$\begin{aligned} \psi &= c'\kappa x^{1/2} F(\xi, \bar{\eta}) \\ T - T_\infty &= (T_0 - T_\infty)\theta(\xi, \bar{\eta}), \\ \bar{\eta} &= \frac{c'y}{x^{1/2}}, \qquad c' = \left[\frac{\rho_\infty g\beta(T_0 - T_\infty)}{\sigma H_0^2 \kappa}\right]^{1/2} \end{aligned} \tag{11}$$

which in (1)–(3) yield

$$\theta - F_{\bar{\eta}} = F_{\bar{\eta}} F_{\bar{\eta}\xi} - F_\xi F_{\bar{\eta}\bar{\eta}} - \frac{1}{2\xi} F F_{\bar{\eta}\bar{\eta}} - \frac{\mathrm{Pr}}{\xi} F_{\bar{\eta}\bar{\eta}\bar{\eta}} \tag{12}$$

$$\theta_{\bar{\eta}\bar{\eta}} + \frac{F}{2}\theta_{\bar{\eta}} = \xi\{F_{\bar{\eta}}\theta_\xi - F_\xi \theta_{\bar{\eta}}\} \tag{13}$$

with boundary conditions

$$\begin{aligned} F = \frac{\partial F}{\partial \bar{\eta}} &= 0; \qquad \theta = 1 \quad \text{on } \bar{\eta} = 0 \\ \frac{\partial F}{\partial \bar{\eta}} &\to 0; \qquad \theta \to 0 \quad \text{as } \bar{\eta} \to \infty. \end{aligned} \tag{14}$$

Equation (12) thus displays not only the anticipated force balance but also the developing inviscid nature of the flow as $\xi \to \infty$, irrespective of Prandtl number. Indeed a reduction of Prandtl number only serves to accentuate this feature of the flow and to highlight the need to introduce an inner viscous layer if boundary conditions at the wall are to be satisfied.

Inverse coordinate expansion solutions of (12) and (13), obtained using similar techniques to those of previous authors, are

$$\begin{aligned} F(\xi, \bar{\eta}) = F_{00}(\bar{\eta}) &- \left(\frac{\mathrm{Pr}}{\xi}\right)^{1/2} + \frac{\gamma^2(1 - \mathrm{Pr})}{2\xi} \ln\frac{\xi}{\mathrm{Pr}} [F_{00}(\bar{\eta}) - \bar{\eta}F'_{00}(\bar{\eta})] \\ &+ \frac{\mathrm{Pr}}{\xi}[F_{02}(\bar{\eta}) + \mu_{02}\{F_{00}(\bar{\eta}) - \bar{\eta}F'_{00}(\bar{\eta})\}] + 0\left(\frac{\mathrm{Pr}}{\xi}\right)^{3/2} \end{aligned} \tag{15}$$

$$\begin{aligned} \theta(\xi, \bar{\eta}) = \theta_{00}(\bar{\eta}) &- \frac{\gamma^2(1 - \mathrm{Pr})}{2\xi} \ln\frac{\xi}{\mathrm{Pr}} [\bar{\eta}F''_{00}(\bar{\eta})] \\ &+ \frac{\mathrm{Pr}}{\xi}[\theta_{02} - \mu\bar{\eta}F''_{00}(\bar{\eta})]. \end{aligned} \tag{16}$$

Here $F_{00}(\bar{\eta})$ and $\theta_{00}(\bar{\eta})$ are solutions of the 0(1) system

$$\begin{aligned} &\theta_{00} - F'_{00} = 0 \\ &\theta''_{00} + \tfrac{1}{2}F_{00}\theta'_{00} = 0. \end{aligned} \tag{17}$$

first examined by Singh and Cowling. Since the order of the system is less than the order of the full equations all the boundary conditions cannot be satisfied. In particular the no slip boundary condition at the boundary is abandoned and (17) solved subject to

$$F_{00}(0) = 0; \qquad F'_{00}(0) = 1; \qquad F'_{00}(\infty) = 0. \tag{18}$$

The numerical solution given by Singh and Cowling is

$$\begin{aligned} &F_{00}(\infty) = 1.616 \\ &F''_{00}(0) = -0.4437 = \gamma \end{aligned}$$

and for small $\bar{\eta}$

$$F_{00}(\bar{\eta}) = \bar{\eta} + \frac{\gamma\bar{\eta}^2}{2!} - \frac{\gamma}{2}\cdot\frac{\bar{\eta}^4}{4!} - \frac{\gamma^2}{2}\frac{\bar{\eta}^5}{3!} + 0(\bar{\eta}^6). \tag{19}$$

Expansion (19) provides the basis for matching conditions on the solutions of an inner viscous layer.

Solutions (15) and (16) display the introduction of logarithmic terms (Stewartson [6]) to ensure exponential decay of $0(\mathrm{Pr}/\xi)$ solutions F_{02}, θ_{02} which remain unsolved. In the special case $\mathrm{Pr} = 1$ no such contributions are necessary. The unknown constant μ_{02} reflects the first indeterminacy of the asymptotic solution associated with the unknown location of the leading edge.

4.2. Inner Layer

Equations valid in the vicinity of the wall where viscous forces are of the same order as those of buoyancy and magnetic drag are obtained from transformations

$$\begin{aligned} \hat{F}(\xi, \hat{\eta}) &= \left(\frac{\xi}{\mathrm{Pr}}\right)^{1/2} F(\xi, \bar{\eta}) \\ \theta(\xi, \hat{\eta}) &= \theta(\xi, \bar{\eta}) \\ \hat{\eta} &= \left(\frac{\xi}{\mathrm{Pr}}\right)^{1/2} \bar{\eta}\ (= H_v y). \end{aligned} \tag{20}$$

The governing equations are

$$\theta - \hat{F}_{\hat{\eta}} + F_{\hat{\eta}\hat{\eta}\hat{\eta}} = \{\hat{F}_{\hat{\eta}}\hat{F}_{\hat{\eta}\hat{\eta}} - \hat{F}_{\xi}\hat{F}_{\hat{\eta}\hat{\eta}}\} \tag{21}$$

$$\theta_{\hat{\eta}\hat{\eta}} = \mathrm{Pr}\,\{\hat{F}_{\hat{\eta}}\theta_{\xi} - \hat{F}_{\xi}\theta_{\hat{\eta}}\} \tag{22}$$

with boundary conditions

$$\begin{aligned} &\hat{F} = \frac{\partial\hat{F}}{\partial\hat{\eta}} = 0; \qquad \theta = 1 \qquad \text{on } \hat{\eta} = 0 \\ &\frac{\partial\hat{F}}{\partial\hat{\eta}} \to 0; \qquad \theta \to 0 \quad \text{as } \hat{\eta} \to \infty. \end{aligned} \tag{23}$$

The solutions consistent with the outer layer solutions are

$$\hat{F}(\xi,\hat{\eta}) = \hat{\eta} - 1 + e^{-\hat{\eta}} + \left(\frac{\Pr}{\xi}\right)^{1/2} \cdot \frac{\gamma\hat{\eta}^2}{2!} - \left(\frac{\Pr}{\xi}\right)^{3/2} \ln\frac{\xi}{\Pr} \cdot \frac{\gamma^3(1-\Pr)}{2\Pr}\frac{\hat{\eta}^2}{2!} + \left(\frac{\Pr}{\xi}\right)^{3/2} \cdot \hat{F}_{13}(\hat{\eta}) + 0\left(\frac{\Pr}{\xi}\right)^2 \tag{24}$$

$$\theta(\xi,\hat{\eta}) = 1 + \left(\frac{\Pr}{\xi}\right)^{1/2} \cdot \gamma\hat{\eta} - \left(\frac{\Pr}{\xi}\right)^{3/2} \ln\frac{\xi}{\Pr}\frac{\gamma^3(1-\Pr)}{2\Pr}\hat{\eta} + \left(\frac{\Pr}{\xi}\right)^{3/2}\theta_{13}(\eta) + 0\left(\frac{\Pr}{\xi}\right)^2 \tag{25}$$

where

$$\hat{F}_{13} = \frac{3\gamma}{2} - \frac{3\gamma}{4}\frac{(1-\Pr)}{\Pr} - \gamma\hat{\eta} + \frac{1}{2}\left[\mu_{13} + \frac{\gamma}{2}\frac{(1-\Pr)}{\Pr}\right]\hat{\eta}^2 - \frac{\gamma}{2}\cdot\frac{\hat{\eta}^4}{4!} + e^{-\hat{\eta}}\left[\frac{3\gamma}{4}\frac{(1-\Pr)}{\Pr} - \frac{3\gamma}{2}\right] + \hat{\eta}\,e^{-\hat{\eta}}\left[\frac{3\gamma}{4}\cdot\frac{(1-\Pr)}{\Pr} - \frac{\gamma}{2}\right] + \frac{\gamma}{4}\frac{(1-\Pr)}{\Pr}\hat{\eta}^2 e^{-\hat{\eta}} \tag{26}$$

and

$$\theta_{13} = \mu_{13}\hat{\eta} - \gamma - \frac{\gamma}{2}\cdot\frac{\hat{\eta}^3}{3!} + \gamma\,e^{-\hat{\eta}} + \frac{\gamma}{2}\hat{\eta}\,e^{-\hat{\eta}}. \tag{27}$$

The unknown constant, μ_{13}, of the inner solution may be related to the indeterminacy of the outer solution via

$$\mu_{13} + \frac{\gamma}{2}\frac{(1-\Pr)}{\Pr} = (F'_{02})_{\bar{\eta}=0} - \mu_{02}\gamma \tag{28}$$

or equivalently

$$\mu_{13} = (\theta'_{22})_{\bar{\eta}=0} - \mu_{02}\gamma. \tag{29}$$

Although the correlation between inner and outer indeterminancies is given above, in the context of coefficients at the plate it is μ_{13} that is of particular interest. Accordingly in the subsequent work it is this quantity alone with which we are concerned. No solutions for F_{02}, θ_{02} are established. The possibility of evaluating μ_{02} once μ_{13} is estimated is simply to be noted. It will be demonstrated that such an estimate may be made from the numerical solution which when incorporated in asymptotic representations of skin friction and heat transfer coefficients gives rise to good agreement with exact results over a large range of ξ.

5. Numerical Solution

A step-by-step numerical solution has been obtained to supplement the series solutions for small and large ξ. Derivatives in the ξ-direction are replaced by differences and all other quantities by averages. The method of solution seeks to establish

velocity and temperature profiles at a station ξ_2, downstream of the station ξ_1, at which profiles are known. These known profiles are used in initial approximations for the averaged quantities of velocity and temperature appearing in two sets of non-linear algebraic equations. An improved approximation for the averaged quantity is obtained using Newton's method and the process repeated until a required accuracy is achieved in the difference between two successive approximations. The solution profiles at ξ_2 are then trivially recovered.

Errors arise from the use of finite differences in both the ξ- and η-directions. The size of truncation errors in the η-direction can be checked using finite difference estimates whilst errors in the ξ-direction are controlled by prescribing a maximum modulus of deviation between a one-step and a two-step solution between ξ_1 and ξ_2. Profiles obtained from integrating over the half interval are the ones used as initial profiles for the next full step of the solution. The level of accuracy achieved is governed solely by the limitations on available storage space. In this instance the integrations in the η-direction were carried out with

$$\eta, \bar{\eta} = 0(0.1)8.0$$

and a maximum modulus of deviation of 10^{-6}. An overall accuracy of at least four decimal places is therefore anticipated.

6. Results

As suggested in § 5 the level of accuracy of the numerical solution is governed by available computer storage. Accordingly in this instance results have been obtained for the case Pr = 0.72 for which the boundary layer width is limited and conditions at infinity are achieved when $\eta \sim 8$ or less. Nevertheless this choice will exemplify the role of logarithmic contributions. Thus the structure evidenced by this investigation will provide a sound basis for a more detailed study of the more practicable case of liquid metals for which Pr $\ll 1$.

Initial profiles for the full numerical solution when the Prandtl number is 0.72, are ϕ_0, θ_0 such that

$$\phi_0''(0) = 0.7967, \qquad \theta_0'(0) = -0.5947. \tag{30}$$

With these profiles system (7) and (8) subject to (9) are integrated as far as $\xi = 4$ where the following correlations hold,

$$\eta = \bar{\eta}; \qquad \frac{\partial F(4, \bar{\eta})}{\partial \bar{\eta}} = 4 \frac{\partial \phi}{\partial \eta}(4, \eta) \tag{31}$$
$$\theta(4, \bar{\eta}) = \theta(4, \eta).$$

After appropriate scaling the numerical solution proceeds using the transformed equations (12) and (13) under boundary conditions (14). Since the skin friction and heat transfer coefficients depend on second velocity derivative and first temperature derivative these quantities as well as velocity and temperature profiles are calculated at each successive ξ-step and then used to evaluate the physical coefficients accordingly.

As the solution marches down the plate the influence of the thickening boundary layer makes it increasingly difficult for the required accuracy to be maintained within the finite interval $0 \leq \bar{\eta} \leq 8$. Integration is therefore terminated at $\xi = 16$ in the anticipation that this will be large enough to be asymptotic in the sense of inner and outer downstream solutions. The numerical details of this integration are presented in Table 1. Illustrative profiles of velocity and temperature in the range $0 \leq \xi \leq 4$ are

Table 1

ξ	τ_w/Pr	Q	ξ	τ_w/Pr	Q	ξ	τ_w/Pr	Q
0.00005	0.0946	4.9869	0.1	0.5722	0.6919	4.1	0.9820	0.1936
0.0001	0.1123	4.1904	0.2	0.6544	0.5641	5.2	1.0000	0.1752
0.001	0.1983	2.3440	0.5	0.7654	0.4227	6.0	1.0101	0.1647
0.002	0.2348	1.9647	1.0	0.8459	0.3335	8.0	1.0288	0.1452
0.005	0.2927	1.5526	1.5	0.8895	0.2878	10.0	1.0418	0.1314
0.01	0.3447	1.2962	2.0	0.9184	0.2581	12.0	1.0515	0.1209
0.02	0.4044	1.0791	3.0	0.9559	0.2201	14.0	1.0591	0.1127
0.05	0.4953	0.8412	4.0	0.9800	0.1956	16.0	1.0651	0.1059

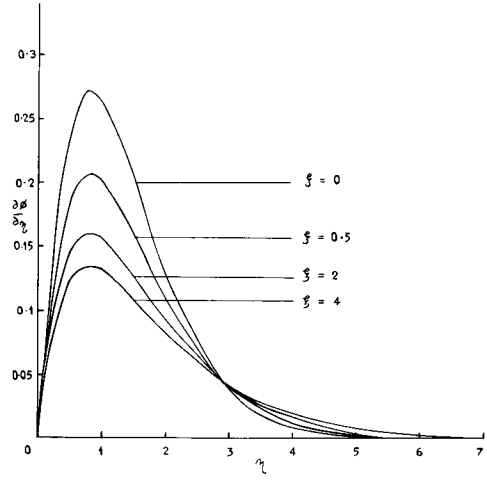

Figure 1
Leading edge velocity profiles.

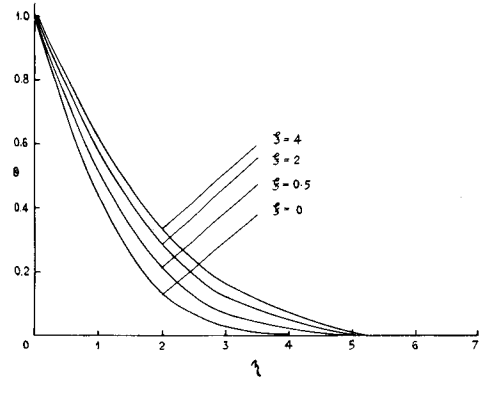

Figure 2
Leading edge temperature profiles.

presented in Figures 1–2. These amply demonstrate the retarding and thickening effects of magnetic drag on the boundary layer. Figure 3 incorporates the full numerical solution profiles at $\xi = 4$ and 16 from the downstream integration together with the zeroth order representations of inner and outer asymptotic solutions.

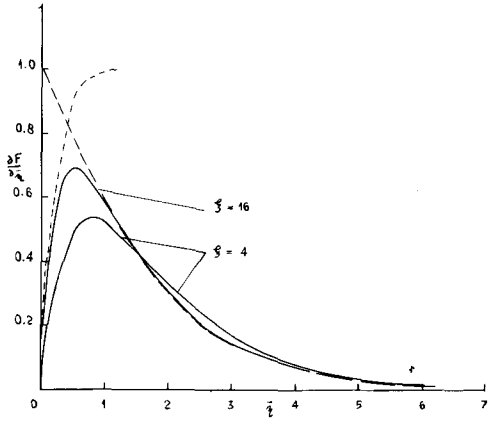

Figure 3
Downstream velocity profiles, —— numerical solutions. — — one term outer. ---- one term inner.

To estimate μ_{13}, the first indeterminacy of the asymptotic solutions, truncated series representation of the temperature first derivative is equated to the exact numerical value at $\xi = 16$. Thus μ_{13} is chosen so that

$$\left\{\frac{\partial\theta}{\partial\bar{\eta}}(\xi,\bar{\eta})\right\}_{\bar{\eta}=0,\ \xi=16} = \left\{\gamma + \frac{\mathrm{Pr}}{\xi}\cdot\mu_{13} + \frac{\mathrm{Pr}}{\xi}\ln\frac{\xi}{\mathrm{Pr}}\left(-\gamma^3\frac{(1-\mathrm{Pr})}{\mathrm{Pr}}\right)\right\}_{\xi=16,\ \mathrm{Pr}=0.72} \tag{32}$$

which yields

$$\mu_{13} = 0.4267. \tag{33}$$

With heat transfer and skin friction coefficients defined by

$$Q = -\left(\frac{\rho_\infty\kappa}{\sigma H_0^2}\right)^{1/2}\frac{1}{T_0 - T_\infty}\left(\frac{\partial T}{\partial y}\right)_{y=0} \tag{34}$$

$$\frac{\tau_w}{\mathrm{Pr}} = \frac{H_0}{g\beta(T_0 - T_\infty)}\left(\frac{\sigma\kappa}{\rho_\infty}\right)^{1/2}\left(\frac{\partial u}{\partial y}\right)_{y=0} \tag{35}$$

truncated series representations are

(a) leading edge

$$Q = 2^{-1/2}\xi^{-1/4}\theta_\eta(\xi,0) = \frac{1}{(4\,\mathrm{Pr}^2\,\xi)^{1/4}}\{-0.5046 + 0.1236\xi^{1/2}\} \tag{36}$$

$$\frac{\tau_w}{\mathrm{Pr}} = 2^{1/2}\xi^{1/4}\phi_{\eta\eta}(\xi,0) = \left(\frac{4\xi}{\mathrm{Pr}^2}\right)^{1/4}\{0.6760 - 0.1880\xi^{1/2}\} \tag{37}$$

(b) downstream

$$Q = -\xi^{-1/2}\theta_{\bar{\eta}}(\xi, 0) = \frac{-1}{\mathrm{Pr}^{1/2}}\,\theta_{\hat{\eta}}(\xi, 0)$$

$$= -\frac{\gamma}{\xi^{1/2}} + \frac{\gamma^3}{\xi^{3/2}}(1 - \mathrm{Pr}) \ln\left(\frac{\xi}{\mathrm{Pr}}\right) - \frac{\mathrm{Pr}}{\xi^{3/2}}\{\mu_{13} - 0.2218\} \tag{38}$$

$$\frac{\tau_w}{\mathrm{Pr}} = \xi^{-1/2} F_{\bar{\eta}\bar{\eta}}(\xi, 0) = \frac{1}{\mathrm{Pr}^{1/2}}\,\hat{F}_{\hat{\eta}\hat{\eta}}(\xi, 0)$$

$$= \frac{1}{\mathrm{Pr}^{1/2}} + \frac{\gamma}{\xi^{1/2}} - \frac{\gamma^3}{2\xi^{3/2}}(1 - \mathrm{Pr}) \ln\left(\frac{\xi}{\mathrm{Pr}}\right) + \frac{\mathrm{Pr}}{\xi^{3/2}}\left\{\mu_{13} - \frac{\gamma}{4\,\mathrm{Pr}}(1 - 3\,\mathrm{Pr})\right\}. \tag{39}$$

These series representations are plotted against the exact solutions in Figures 4 and 5.

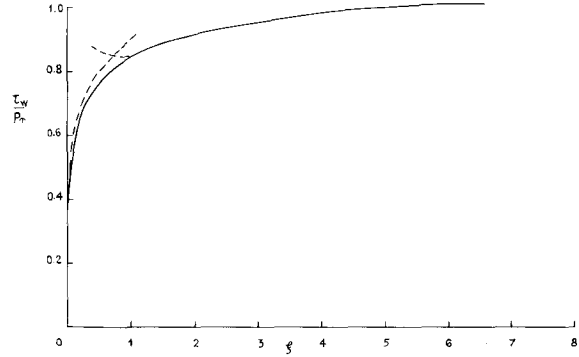

Figure 4
Skin friction coefficient, —— numerical solution, ---- series representations.

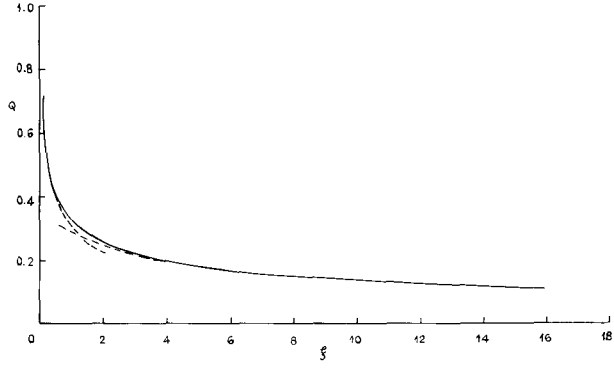

Figure 5
Heat transfer coefficient, —— numerical solution, ---- series representations.

7. Discussion

A detailed investigation of the title problem has been outlined. With the given estimate of μ_{13} a high level of agreement is demonstrated between the exact numerical

solution and series estimates. In both cases of heat transfer and skin friction coefficients estimates overlap over almost the whole range of ξ. Moreover the points at which series representations diverge from the correct solutions are such as to give some confidence that straightforward extrapolations linking these series representations may well be sufficient for practical purposes for 0(1) values of the Prandtl number.

Of particular note is a comparison of the relative magnitudes of the second and third terms of (38) and the third and fourth terms of (39). Here the knowledge of the asymptotic structure including the logarithmic terms is particularly significant. For Pr of 0(1), the algebraic term dominates whereas as the Prandtl number decreases into the range where significant effects may be observed in practice, i.e. in the context of liquid metals, it is the logarithmic term which will provide the dominant higher order correction to skin friction and heat transfer estimates. Although the variation of μ_{13} with Prandtl number remains an open question it is doubtful that such variation will affect the validity of this feature.

References

[1] K. R. SINGH and T. G. COWLING, Quart. J. Mech. and Appl. Math. *16*, 1, 1963.
[2] E. M. SPARROW and R. D. CESS, Int. J. Heat Mass Trans. *3*, 267, 1961.
[3] N. RILEY, J. Fluid Mech. *18*, 577, 1964.
[4] H. K. KUIKEN, J. Fluid Mech. *40*, 21, 1970.
[5] S. OSTRACH, N.A.C.A. Rep. 1111, 1953.
[6] K. STEWARTSON, J. Maths. Phys. *36*, 173, 1957.

Summary

The magnetohydrodynamic free convection flow of an electrically conducting fluid past a semi-infinite plate in a strong cross-field has been examined. Formulation in terms of a characteristic length has enabled a full numerical solution to be obtained providing details of skin friction and heat transfer at all stations along the plate. An estimate of an indeterminacy in asymptotic solutions allows favourable comparison to be made between series solutions estimates of these quantities and their exact numerical values.

Zusammenfassung

Die magneto-hydrodynamische Strömung mit freier Konvektion in einer elektrisch leitenden Flüssigkeit entlang einer halbunendlichen Platte ist in einem starken Querfeld untersucht worden. Die Einführung einer charakteristischen Länge hat eine vollständige numerische Lösung ermöglicht, die die Reibungskraft und den Wärmeübergang entlang der Platte ergibt. Eine Abschätzung von einer Unbestimmtheit in den asymptotischen Lösungen erlaubt einen Vergleich zwischen den durch Reihelösungen erhaltenen Werten dieser Grössen und ihren exakten numerischen Werten.

(Received: February 16, 1976)